



Sonoelectrochemical synthesis of metal-organic frameworks



Gilvaldo G. da Silva^{a,1}, Cecília S. Silva^{a,1}, Rogério T. Ribeiro^b, Célia M. Ronconi^c,
Bráulio S. Barros^d, Jorge L. Neves^{a,*}, Severino Alves Júnior^{a,*}

^a Department of Fundamental Chemistry, UFPE, 50740-560 Recife, PE, Brazil

^b Department of Biophysics, UFPE, 50740-560 Recife, PE, Brazil

^c Department of Inorganic Chemistry, UFF, 24020-150, Niterói, RJ, Brazil

^d Department of Mechanical Engineering, UFPE, 50740-560 Recife, PE, Brazil

ARTICLE INFO

Article history:

Received 1 March 2016

Received in revised form 21 June 2016

Accepted 4 July 2016

Available online xxx

Keywords:

HKUST-1

Cu-BTC

Sonoelectrochemical

ABSTRACT

Here we report a new synergic strategy for the synthesis of metal-organic frameworks (MOFs), the sonoelectrochemical method. The metal-organic framework HKUST-1 $[\text{Cu}_3(\text{BTC})_2(\text{H}_2\text{O})_3]_n$ was successfully prepared by using this approach. Structural and morphological properties of HKUST-1 were studied and results compared with those obtained for the same material synthesized via a conventional solvothermal method. The sonoelectrochemical approach allowed the preparation of powder samples with nanosized characteristics, high yields and in a short time. Furthermore, we confirmed that this route worked well for the synthesis of others MOFs, such as ZIF-8 and MIL-53. Such simple and practical strategy may allow the large-scale production of MOFs, which is of great interest for industrial applications.

© 2016 Published by Elsevier B.V.

1. Introduction

Metal-Organic Frameworks (MOF) have become very attractive for industrial applications in the past years due to its unique properties such as the high thermal stability, the high porosity, and absence of any dead volume just to give some examples [1]. The great interest in this kind of material has driven the search and development of new synthetic strategies allowing large-scale production with low-cost and high-yield. Thereby, several synthetic routes have been employed during the last decades, such as slow diffusion, hydro(solvo)thermal, ionothermal, free solvent, sonochemistry, mechanochemistry, and electrochemistry [2–13].

However, these techniques are more suitable for the lab scale, so the development of synthetic routes in industrial scale is still necessary. As an alternative, it seems possible to explore the synergistic effect observed when combining two different synthetic approaches, such as sonochemistry and electrochemistry. The sonoelectrochemistry route is a straightforward and easy technique with well-established foundations and widely applied in

electrodeposition, organic synthesis, and preparation of nanoparticles [14–16].

The metal-organic framework HKUST-1 $[\text{Cu}_3(\text{BTC})_2(\text{H}_2\text{O})_3]_n$ (BTC = 1,3,5-benzenetricarboxylate) is one of the most widely studied MOFs [17–21]. This MOF presents large surface area, high pore volume, high chemical stability and also the ability to bind water, among other molecules, by coordinating to the unsaturated Cu(II) sites [17]. These properties combined with the high structural stability upon water adsorption/desorption makes HKUST-1 a very promising candidate for gas storage, catalysis and sensing applications [22–26]. In addition to direct applications of HKUST-1 can notice a significant number of investigations in the development of composite materials based on these types of MOFs with the purpose of enhancing and expand the application range [27–29]. The main structural feature of HKUST-1 is a monomeric unit containing dinuclear clusters (paddle wheel) with a square-based pyramidal geometry and copper-copper distance of about 2.63 Å. Twelve oxygen atoms, from the carboxylate groups of the four BTC ligands, bind to the four coordination sites of each of the three Cu^{2+} ions [17].

In this scenario, we present a synthetic route to prepare the HKUST-1 using a sonoelectrochemical method. Despite the need for sophisticated equipment, the increase in the yield as well as the decrease in reaction time, besides milder electrochemical conditions, certainly justify the utilization of this approach. To the best

* Corresponding authors.

E-mail addresses: jorge.lneves@ufpe.br (J.L. Neves), salvesjr@ufpe.br (S.A. Júnior).

¹ Both authors contributed equally to this work.

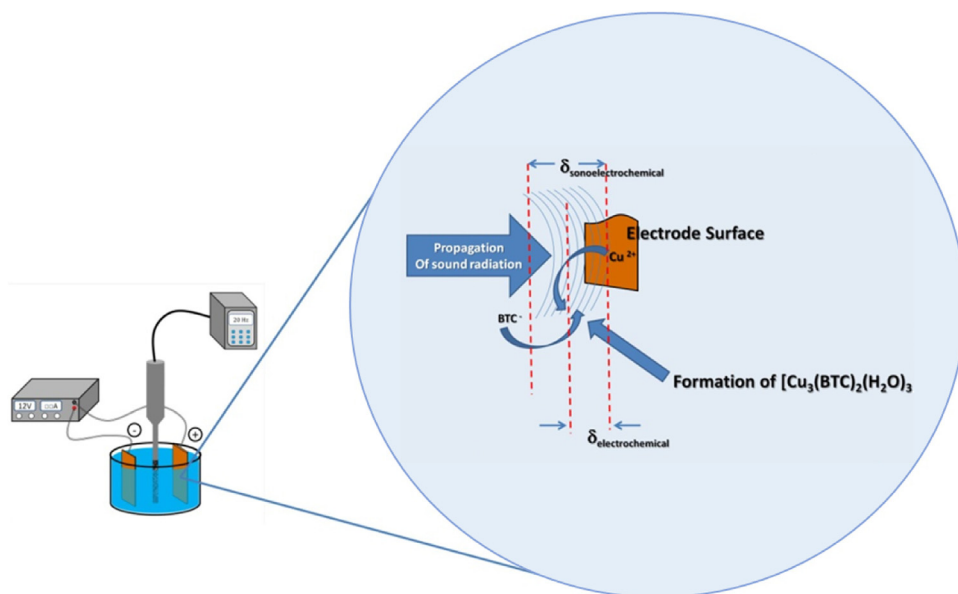


Fig. 1. Illustration of the behavior of the diffuse layer (δ) regarding the method (electrochemical or sonoelectrochemical) used in the formation of HKUST-1. Also is schematized the increase gradient of temperature (T) and pressure (P) with the distance x of propagation of sound radiated.

of our knowledge, this is the first time that such strategy is used to synthesize MOFs.

The use of two electrodes (without the reference electrode) enables the simple and easy application of the sonoelectrochemistry route for large-scale production of HKUST-1. As a result, this new configuration shows a synergistic effect that promotes an increase in the yields and reduction in synthesis time.

2. Materials and methods

2.1. Synthesis

2.1.1. Reactants

1,3,5-Benzenetricarboxylic acid (95.0%), NaNO_3 (99.0%) and dimethylformamide (DMF) (99.8%), purchased from Aldrich (USA), were used as received and without further purification.

2.1.2. Working electrode

The working electrode (anode), a copper wire with a diameter of 0.133 cm, was previously polished using sandpaper granulometry 1200, immersed in a nitric acid solution (20% v/v) for two minutes and rinsed out with detergent.

2.1.3. Sonoelectrochemical synthesis

In a typical process, NaNO_3 (0.24 mol L^{-1}) and 1,3,5-Benzenetricarboxylic acid (24 and 48 mmol L^{-1}) were dissolved in a mixture of DMF/ H_2O solvents (1:1, v/v). The resulting solution placed into a single-compartment electrochemical cell with two copper electrodes partially immersed. An electrical potential difference was applied between the electrodes, initiating the process of anodic dissolution ($\text{Cu}^0_{(\text{aq})} \rightleftharpoons \text{Cu}^{2+}_{(\text{aq})} + 2e^-$), while the solution was kept under ultrasonic irradiation to ensure the expected synergic effect. This process, together with the deprotonation of trimesic acid ($\text{H}_3\text{BTC}_{(\text{aq})} + 3 \text{ DMF}_{(\text{aq})} \rightleftharpoons \text{BTC}^{3-}_{(\text{aq})} + 3 \text{ HDMF}^+_{(\text{aq})}$) allowed the formation of a blue precipitate (HKUST-1). The Table S1 displays the experimental conditions for SE(1)–(8) assays. A DC POWER SUPPLY (model FA-3005-INTRUSTHERM) was used to generate electrical potential difference (12 V). A Sonic-Vibra-Cell™ apparatus generated the ultrasound frequency (20 KHz, 30 and 60% of power).

All products were washed with water (2×), ethanol/acetone 1:1 (3×) and then dried at room temperature.

2.2. Characterization

Powder X-ray diffraction (XRD) analyses were performed in a SHIMADZU equipment, model XRD-7000, equipped with Cu Tube ($K\alpha$ of 1.542 \AA) operating at 40 kV and 30 mA and using the following Slits: S = 1 deg, SS = 1 deg, e RS = 0.3 nm. The pore volume and surface area were obtained by using the BET method. All samples were previously dried at 90°C for 16 h. About 50 mg of each sample placed into a quartz cell attached to the physisorption apparatus (Micromeritics ASAP 2010) to dry under vacuum at 100°C for 2 h and then the nitrogen adsorption isotherms were measured at 77.4 K. The FT-IR spectra ($4000\text{--}400 \text{ cm}^{-1}$) have been achieved with a resolution of 2 cm^{-1} at room temperature on a Bruker Tensor-27 spectrometer, fitted with a DTGS detector. The samples were previously prepared as KBr mixtures and recorded through the ATR technique. The thermogravimetric analyses were performed under N_2 atmosphere at a rate of $10^\circ\text{C}/\text{min}$ in a Shimadzu apparatus, model DTG-60. The samples were heated from room temperature up to 800°C . The particle morphology was examined by using Scanning Electron Microscopy (SEM) in a JEOL/JSM-5900 apparatus. For Transmission Electron Microscopy (TEM) analysis was used an FEI Morgani 268D equipment, 80–100 kV, Eindhoven, Netherlands.

3. Results and discussion

We study the effect of experimental parameters, such as the ultrasound power, the reaction time, and the ligand concentration, on the HKUST-1 synthesis. With this purpose, eight different experimental combinations were prepared (Table S1, see ESI³). A careful analysis of these data suggests that the ultrasound power, the reaction time, and consequently the current density are most relevant parameters when compared to ligand concentration. By

³ Electronic Supplementary information (ESI) available: PXRD, BET, TGA, TEM and IV data.

increasing the ultrasound power, the crystallite size decreases suggesting that the ultrasound waves interfere in the growth of the crystallites. At the same time, the current density increases, as well as the yields. The high yields obtained here for the sono-electrochemical synthesis of HKUST-1 are associated with the acoustic cavitation phenomenon (transient bubbles at high pressure and temperature), and your strong influence on the diffusion process of species (bulk solution) to the electrode surface. Since the sono-electrochemical system behaves as a hydrodynamic electrode (Fig. 1), the thickness of the diffuse double layer (δ) decreases and it allows a high diffusion of reactive species (benzenetricarboxylic acid) on the next to surface (the region in which the reaction occurs) [30,31]. The formation of acoustic cavitation in the interface region (electrode/solution) is easier than in homogeneous medium due to surface irregularities (e.g. roughness, cracking) and the results are superior to the separated processes [32].

The XRD pattern of the sample prepared via sono-electrochemistry route matches well with patterns of HKUST-1 obtained via the hydrothermal method and simulated for a cubic structure with SG: Fm-3m (Fig. 2) [33,34]. The simulated patterns were calculated based on crystal structure data of HKUST-1 as-prepared, with solvent molecules into the pores, and activated (solvent removed). The relative ratio intensities of the diffraction peaks at 6.70° (002) and 11.62° (222) in the diffraction pattern of the sample prepared by sono-electrochemistry method suggest the presence of solvent molecules into the pores. It is worth to mention that the type and amount of solvent into the pores of MOF's may affect the relative intensities of the diffraction peaks.

N_2 adsorption-desorption isotherm at 77.4 K of HKUST-1 prepared by sono-electrochemical route is displayed in Fig. S2 (see ESI). The curves obtained suggest a combination of isotherms type I and type IV according to IUPAC classification [35]. It is also noticeable a hysteresis loop that can be classified as a mixture of types H3 and H4 which is an indicative of both aggregate particles and microporosity [35]. The initial part of the sorption isotherms is related to adsorption isotherm of Type I, indicating micropore filling at low pressures. At high pressures ($P/P_0 > 0.9$) the shape of the curves suggests a Type IV isotherm that can be related either to mesopores or large pores due to intraggregative voids. Type H4 hysteresis supports this latter possibility. Kim et al. obtained

similar isotherms for Cu-BTC prepared by a continuous-flow microreactor-assisted solvothermal system [36]. Calculation of the surface area and pore volume from the N_2 adsorption isotherm was performed for SE(8) sample and their corresponding values are 403.8 and $541.0 \text{ m}^2 \text{ g}^{-1}$ of BET and Langmuir surface areas, respectively, and single point total pore volume = $0.332 \text{ cm}^3 \text{ g}^{-1}$. The reduced porosity value can be assigned the presence of sodium nitrate in the cavities, as noted in the PXRD analyses (Fig. S1, see ESI), besides of the no-activation of sample as a post-synthesis procedure [37].

SEM images reveal an unambiguous influence of the synthetic route on size and morphology of the particles. Powders prepared via sono-electrochemical method exhibit small particles size ($< 500 \text{ nm}$) with both quasi-spherical and octahedral shapes (Figs. 3A and S5). While that, the powder prepared by conventional solvothermal method presents microcrystals with size around 2–15 μm and a typical octahedral habit. Additionally, the average crystallite size was calculated based on the broadening of the diffraction peaks at 6.70° (002), 9.48° (022), 11.62° (222) and 13.42° (004) using the Scherrer's equation. The samples present crystallite sizes in the interval of 22–47 nm (Table S1, see ESI) indicating that the particles have a polycrystalline character. These results suggest that sono-electrochemical synthesis is an advantageous way to get nanocrystals compared to the conventional solvothermal method.

Ultrasound-assisted synthesis methods involve the cavitation process, which is the formation, growth, and implosive collapse of bubbles in a liquid, generating local hot spots having temperatures up to 5000°C , 500 atm pressures with a lifetime of a few microseconds [38–40]. Such extreme conditions may increase the number of crystallization nuclei leading to the formation of nanosized structures [41].

We applied the Bravais-Friedel-Donnay-Harker (BFDH) method to simulate the morphology and rationalize the growth of the crystals of HKUST-1 [42,43]. Calculations were performed starting from crystallographic data with Mercury 3.7 software [44]. The BFDH method provides an approximated crystal morphology by assuming that the facets most energetically stable and with slowest growing are the ones with the largest interplanar spacing [45]. The growth rate R_{hkl} of a crystalline plane (hkl) at the normal direction is inversely proportional to the inter-planar spacing, d_{hkl} [45].

The simulated morphology was a cubo-octahedron with exposed facets {111} and {002}. We suggest that this habit can be easily confused with a spherical shape due to the nanocrystal size (Figs. 3A and S5, see ESI). Due to $d_{\{111\}} > d_{\{002\}}$, the relationship between the growth rates is $R_{\{111\}} < R_{\{002\}}$ what explain why the fastest growing facets {002} show lower total surface area than facets {111}. Extrapolating the growth rate of facets {002} is possible to demonstrate the octahedral habit of microcrystals prepared by the hydrothermal method, in which facets {111} dominates the morphology (Fig. 3C). According to Umemura et al. [46], for the HKUST-1 structure, the most favourable and faster growth process occurs along to the (100) direction, resulting in the octahedral morphology. We assume that the great number of crystallization nuclei formed during sono-electrochemical synthesis, due to the cavitation effect, may limit the crystal growth keeping the cubo-octahedron habit.

The IR spectrum of HKUST-1 (Fig. S3, see ESI) displays two strong bands, ν_{as} (COO⁻) and ν_s (COO⁻), at 1645 cm^{-1} and 1385 cm^{-1} , respectively. The difference between wavenumbers of asymmetric and symmetric stretching vibrations provides information about the coordination mode of the carboxylate group. In this case, $\Delta\nu = 260 \text{ cm}^{-1}$ suggests the *syn-syn* bidentate bridging mode of COO⁻ groups what is in agreement with the structure of HKUST-1. Broadband at around 3500 cm^{-1} corresponding to the

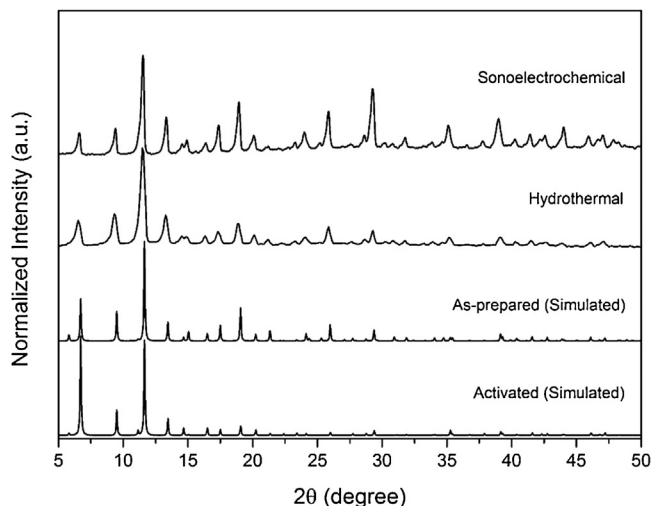


Fig. 2. (a) PXRD pattern of HKUST-1 synthesized via sono-electrochemical method, (b) digitalized PXRD pattern of HKUST-1 obtained via hydrothermal method by Hartmann et al. [33], (c) simulated PXRD patterns of HKUST-1 as-prepared and (d) activated. The simulated patterns were generated by Mercury 3.7 software based on crystal structure data reported by Yakovenko et al. [34].

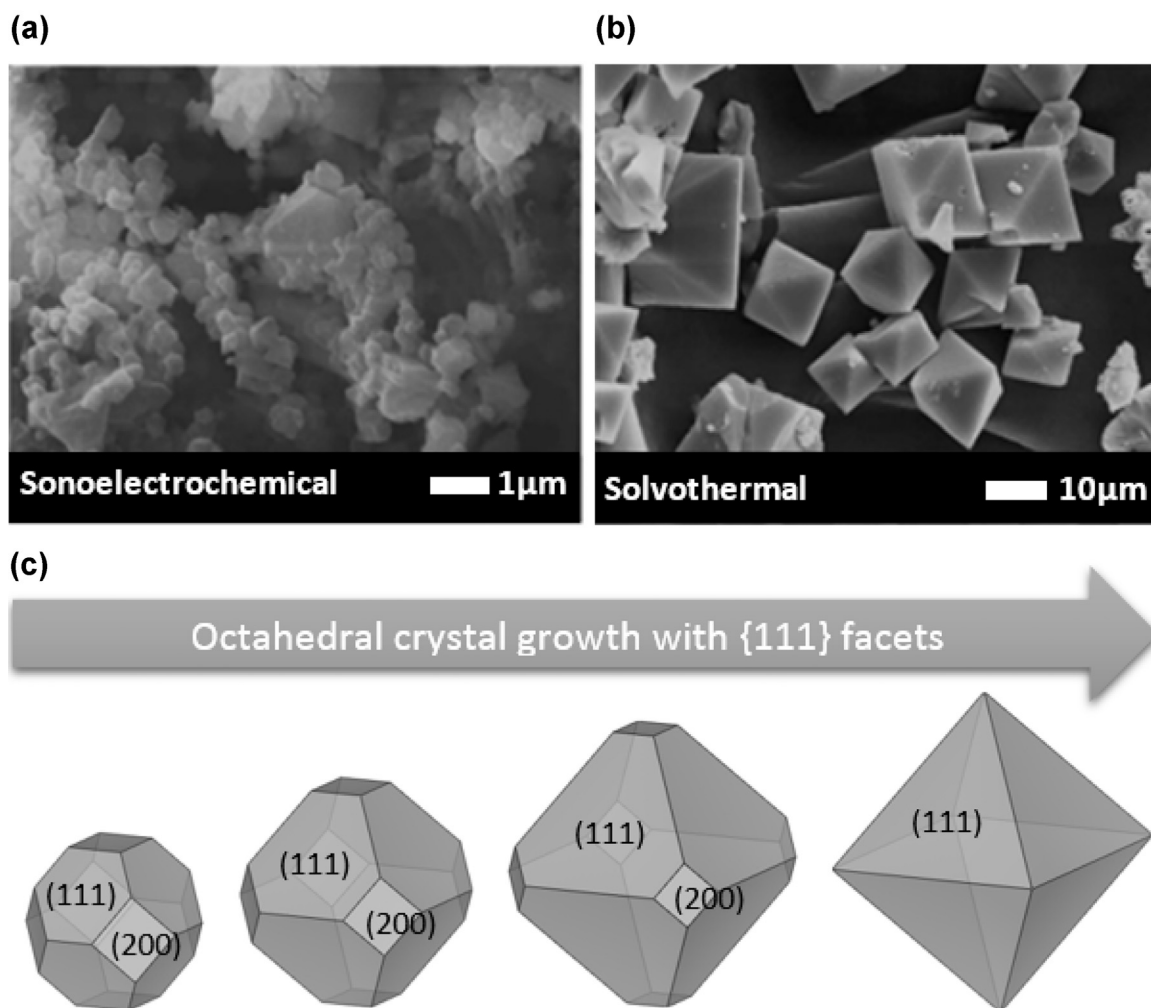


Fig. 3. SEM images of the MOF obtained by (a) sonoelectrochemical and (b) solvothermal synthesis. (c) Crystal growth simulated according to BFDH model [42,43].

stretching vibration of O–H bond indicates the presence of water molecules in the sample [47].

The thermal stability was studied using TGA (Fig. S4, see ESI). Three distinct mass loss events are observed. The first one up to 100 °C attributed to the loss of hydration water while the second one from 100 up to 200 °C assigned to the coordinated water loss. Finally, the last event ascribed to the decomposition of the organic ligand around 300 °C leading to the formation of copper oxide.

In addition to the present study, the sonoelectrochemical method was used to prepare MOFs based on Zn and Al metals, in combination with the linkers imidazole and terephthalic acid, respectively. The XRD patterns of the prepared MOFs agree well with the simulated patterns calculated from crystallographic data (Fig. S6, see ESI) [48,49]. Therefore, we observed that was possible an extrapolation of the method for synthesis of another MOFs.

4. Conclusions

In summary, we have presented a new strategy, the electrochemical method, for the synthesis of metal-organic frameworks, based on the synergistic effect observed when combining two different synthetic approaches, sonochemistry and electrochemistry. Analysis of the obtained powder samples by XRD confirmed the formation of the desired metal-organic structures, HKUST-1, MIL-53 and ZIF-8 with high yields and in a very short time compared to conventional methods. Besides, electron microscopy analysis revealed the nanosized characteristics of HKUST-1 by the

sonochemical method. On the other hand, HKUST-1 powder prepared by the conventional solvothermal method presented tetrahedral microcrystals. To the best of our knowledge, this is the first time that such strategy was used to synthesize MOFs. We expect that this new approach may open new opportunities for large-scale production and industrial applications.

Acknowledgements

The authors would like to acknowledge the Brazilian funding agencies CNPq (process no. 407445/2013-7), CAPES, FACEPE and INCT-INAMI research network. We are in debt with prof. Marcelo Navarro, who has provided support on the electrochemical setup and Sergio Santos for helping in the improvement of the SEM images.

Appendix A. Supplementary data

Supplementary data associated with this article can be found, in the online version, at <http://dx.doi.org/10.1016/j.synthmet.2016.07.003>.

References

- [1] A.U. Czaja, N. Trukhan, U. Mueller, *Chem. Soc. Rev.* 38 (2009) 1284–1293.
- [2] X. Chen, B. Zhao, W. Shi, J. Xia, P. Cheng, D. Liao, S. Yan, Z. Jiang, *Chem. Mater.* 17 (2005) 2866–2874.

- [3] O. Yaghi, H. Li, *J. Am. Chem. Soc.* 117 (1995) 10401–10402.
- [4] E.R. Parnham, R.E. Morris, *Acc. Chem. Res.* 40 (2007) 1005–1013.
- [5] A. Pichon, A. Lazuen-Garay, S. James, *CrystEngComm* 8 (2006) 211–214.
- [6] W.-J. Son, J. Kim, J. Kim, W.-S. Ahn, *Chem. Commun.* (2008) 6336–6338.
- [7] D. Braga, M. Curzi, A. Johansson, M. Polito, K. Rubini, F. Grepioni, *Angew. Chem. Int. Ed.* 45 (2006) 142–146.
- [8] A.M. Joaristi, J. Juan-Alcaniz, P. Serra-Crespo, F. Kapteijn, J. Gascon, *Cryst. Growth Des.* 12 (2012) 3489–3498.
- [9] J. Kulesza, B.S. Barros, I.M.V. da Silva, G.G. da Silva, S. Alves-Júnior, *CrystEngComm* 15 (2013) 8881–8882.
- [10] M. Li, M. Dincă, *Chem. Mater.* 27 (2015) 3203–3206.
- [11] M. Li, M. Dincă, *Chem. Sci.* 5 (2014) 107–111.
- [12] M. Li, M. Dincă, *J. Am. Chem. Soc.* 133 (2011) 12926–12929.
- [13] A. Doménech, H. García, M.T. Doménech-Carbó, F. Llabrés-i-Xamena, *Electrochem. Commun.* 8 (2006) 1830–1834.
- [14] A. Durant, J. Delplancke, V. Libert, J. Reisse, *Eur. J. Org. Chem.* (1999) 2845–2851.
- [15] A. Gedanken, *Ultras. Sonochem.* 11 (2004) 47–55.
- [16] I. Haas, A. Gedanken, *Chem. Commun.* (2008) 1795–1797.
- [17] S. Loera-Serna, M.A. Oliver-Tolentino, M.L. López-Núñez, A. Santana-Cruz, A. Guzmán-Vargas, R. Cabrera-Sierra, H.I. Beltránand, J. Flores, *J. Alloys Compd.* 540 (2012) 113–120.
- [18] S. Chui, S. Lo, J. Charmant, A. Orpen, I. Williams, *Science* 283 (1999) 1148–1150.
- [19] C. Chiericatti, J.C. Basilico, M.L.Z. Basilico, J.M. Zamaro, *Microporous Mesoporous Mater.* 162 (2012) 60–63.
- [20] M.V. Parkes, H. Demir, S.L. Teich-McGoldrick, D.S. Sholl, J.A. Greathouse, M.D. Allendorf, *Microporous Mesoporous Mater.* 194 (2014) 190–199.
- [21] T. Toyao, K. Liang, K. Okada, R. Ricco, M.J. Styles, Y. Tokudome, Y. Horiuchi, A.J. Hill, M. Takahashi, M. Matsuoka, Paolo Falcaro, *Inorg. Chem. Front.* 2 (2015) 434–441.
- [22] X. Zhao, S. Liu, Z. Tang, H. Niu, Y. Cai, W. Meng, F. Wu, J. P. Giesy, *Scientific Reports*, 5 (2015) 11849, 1–10.
- [23] K. Schlichte, T. Kratzke, S. Kaskel, *Microporous Mesoporous Mater.* 73 (2004) 81–88.
- [24] H. Dathé, E. Peringer, V. Roberts, A. Jentys, J. Lercher, *C. R. Chim.* 8 (2005) 753–763.
- [25] L.E. Kreno, K. Leong, O.K. Farha, M. Allendorf, R.P. Van Duyne, J.T. Hupp, *Chem. Rev.* 112 (2012) 1105–1125.
- [26] Q. Zhu, Y. Chen, W. Wang, H. Zhang, C. Ren, H. Chen, X. Chen, *Sens. Actuators B* 210 (2015) 500–507.
- [27] M.R. Lohe, K. Gedrich, T. Freudenberg, E. Kockrick, T. Dellmann, S. Kaskel, *Chem. Commun.* 47 (2011) 3075–3077.
- [28] A. Ahmed, M. Forster, R. Clowes, D. Bradshaw, P. Myers, Haifei Zhang, *J. Mater. Chem. A* 1 (2013) 3276–3286.
- [29] M.S. Pinto, C.A. Sierra-Avila, J.P. Hinestroza, *Cellulose* 19 (2012) 1771–1779.
- [30] E. Cooper, L. Coury, *J. Electrochem. Soc.* 145 (1998) 1994–1999.
- [31] F. Marken, R. Akkermans, R. Compton, *J. Electroanal. Chem.* 415 (1996) 55–63.
- [32] R. Chow, R. Blindt, R. Chivers, M. Povey, *Ultrasonics* 41 (2003) 595–604.
- [33] M. Hartmann, S. Kunz, D. Himsl, O. Tangermann, *Langmuir* 24 (2008) 8634–8642.
- [34] A.A. Yakovenko, J.H. Reibenspies, N.H.-C. Bhuvanesh. Zhou, *J. Appl. Cryst.* 46 (2013) 346–353.
- [35] K. Sing, *Pure Appl. Chem.* 54 (1982) 2201–2218.
- [36] K.J. Kim, Y.J. Li, P.B. Kreider, C.H. Chang, N. Wannenmacher, P.K. Thallapally, H. G. Ahnd, *Chem. Commun.* 49 (2013) 11518–11520.
- [37] N.A. Janabi, P. Hill, L.T. Murciano, A. Garforth, P. Gorgojo, F. Siperstein, X. Fan, *Chem. Eng. J.* 281 (2015) 669–677.
- [38] R. Feng, Y. Zhao, C. Zhu, T.J. Mason, *Ultras. Sonochem.* 9 (2002) 231–236.
- [39] M. Strasberg, *J. Acoust. Soc. Am.* 31 (1959) 163–176.
- [40] K. Negishi, *J. Phys. Soc. Jpn.* 16 (1961) 1450–1465.
- [41] D. Tanaka, A. Henke, K. Albrecht, M. Moeller, K. Nakagawa, S. Kitagawa, J. Groll, *Nat. Chem.* 2 (2010) 410–416.
- [42] J.D.H. Donnay, D. Harker, *Am. Mineral.* 22 (1937) 446.
- [43] J. Prywer, *J. Cryst. Growth* 270 (2004) 699–710.
- [44] C.F. Macrae, P.R. Edgington, P. McCabe, E. Pidcock, G.P. Shields, R. Taylor, M. Towler, J. van de Streek, *J. Appl. Cryst.* 39 (2006) 453–457.
- [45] Hui Xu, Xingtang Rao, Junkuo Gao, Jiancan Yu, Ziqi Wang, Zhongshang Dou, Yuanjing Cui, Yu Yang, Banglin Chen, Guodong Qian, *Chem. Commun.* 48 (2012) 7377–7379.
- [46] A. Umemura, S. Diring, S. Furukawa, H. Uehara, T. Tsuruoka, S. Kitagawa, *J. Am. Chem. Soc.* 133 (2011) 15506–15513.
- [47] Y.-K. Seo, G. Hundal, I.T. Jang, Y.K. Hwang, C.-H. Jun, J.-S. Chang, *Microporous Mesoporous Mater.* 119 (2009) 331–337.
- [48] T. Loiseau, C. Serre, C. Huguénard, G. Fink, F. Taulelle, M. Henry, T. Bataille, G. Fjrey, *Chem. Eur. J.* 10 (2004) 1373–1382.
- [49] Y. Pan, D. Heryadi, F. Zhou, L. Zhao, G. Lestari, H. Sub, Z. Lai, *CrystEngComm* 13 (2011) 6937–6940.